Rheology of Poly(vinyl chloride) Plastisol for Super-High-Shear-Rate Processing. II

N. Nakajima,[1] E. R. Harrell[2]

[1]*Institute of Polymer Engineering, The University of Akron, Akron, Ohio 44325-3909*
[2]*PolySciCon, LLC, Avon Lake, Ohio 44012*

ABSTRACT: Capillary flow of poly(vinyl chloride) plastisol was examined at low, high, and superhigh shear rates. At the low to intermediate shear rates, the flow was pseudo-plastic, but the measured viscosity was not reproducible and widely scattered. The flow behavior was explained as the breakup of the particle network into network-fragments of varying size. At high shear rates, the measured viscosity was reproducible and increased with shear rate, indicating that the particles were, by and large, separated from each other. At superhigh shear rates, the viscosity decreased with the increase of shear rate. The particles cease to participate in flow because rotation becomes more difficult. A plug-flow ensues with a thin layer of lubricating plasticizer. © 2011 Wiley Periodicals, Inc. J Appl Polym Sci 123: 1377–1383, 2012

Key words: colloids; poly(vinyl chloride) (PVC); processing; rheology

INTRODUCTION

There are two routes for preparing flexible products from plasticized poly(vinyl chloride) (PVC). One is to use premixes in solid form, and the other is to use premixes in liquid form. The solid premixes are made by thermomechanically blending PVC with plasticizer and pelletizing or letting plasticizer be absorbed into the pores of the resin, resulting in a free-flowing powder. The premixes are fabricated with the same equipment (for extrusion, injection molding, etc.) as those used for other thermoplastic resins. The resin for this route is suspension-polymerized in an aqueous medium in the presence of a suspending agent, giving a powder of approximately 100-μm particle size. The liquid premixes are prepared by mixing the resin powder with plasticizer, giving a paste called *plastisol*.[1,2] The resin is polymerized in the aqueous medium in the presence of emulsifier. After the polymerization, the aqueous emulsion is spray-dried to give spherical particles (primary particles) of about 1-μm diameter with a minor amount of smaller size particles. The spray-drying also creates agglomerated particles consisting of primary particles. The agglomerated particles are ground to a size smaller than 15 μm. The ground particles are nonspherical.[3] The resin particle contains emulsifier (used for polymerization), the type of which affects performance of the plastisol.[4]

The rheology of plastisol processing encompasses two aspects. One is a suspension rheology, which is related to spreading or coating of the material on the substrate at room temperature. The other is gelation and fusion, which takes place by heating in an oven.[5] The present work is concerned with the former.

The plastisol, being liquid, can be fabricated by a variety of processes, but a major advantage is in coating processes. The higher coating speed increases productivity, and the thinner coating results in material saving. Both requirements are ever present for maintaining economic competitiveness. The combination of the higher speed and thinner coating results in a higher shear rate. However, there is generally considered to be a limit of shear rate because the flow becomes unstable and the coating might even tear with the increasing shear rate. In analogy to the superhigh-shear-rate processing of high-density polyethylene (which is extruded at shear rates higher than the instability region), it is thought that plastisol may also be processed at the superhigh shear rate if the instability is made to occur inside of the die assembly.[6] For simulating the situation, a capillary rheometer is suitable because the plastisol flows through a completely closed channel. Rotational rheometer geometries are open at the edge. Our past study showed that at the higher shear rates, plastisol tended to go towards the opening of the coaxial cylinder rheometer.[7] At even higher shear rates, the liquid sample is

expelled from the opening, such that rheological measurements are not possible.

In the pioneering work by Hoffman,[8] steady-state viscosity–shear rate curves are shown for a model plastisol at several concentrations between 0.47 and 0.57 volume fraction of particles. Measurements were made with either cone-plate or parallel-plate rheometry. The curves consist of pseudo-plastic region at the lower shear rate, reaching a minimum viscosity and, then, dilatant behavior at the intermediate shear rate. With volume fractions of 0.47 and 0.49, the viscosity goes over a maximum and then decreases at the higher shear rate region. With higher concentrations, 0.51, 0.55, and 0.57, the viscosity curves break after the dilatant behavior, and the viscosity jumps to very high values.

In our earlier paper,[9] the pseudo-plastic behavior was interpreted as the result of the stress-induced phase separation into an immobilized layer and a mobile phase. The immobilized layer grows with the increase of shear rate. Consequently, the particle concentration of the mobile phase decreases, resulting in the decrease of viscosity.

The dilatant behavior was explained as the result of the dilatation of the immobilized layer. When the dilatation exceeds the limit of strength, the layer fractures. Both the break of the viscosity curve and the viscosity maximum were interpreted as the result of a failure of the immobilized layer.[10]

In our more recent observation with a commercial plastisol, having a 52.8% volume fraction of particles, the steady-state viscosity–shear rate relation measured with a coaxial cylinder rheometer showed a maximum at the higher shear rate.[11] With the viscosity curve alone, it is difficult to unequivocally call the maximum a failure point. However, the accompanying measurement of normal stress and visual observation indicated an onset of instability.[11]

The present work is to examine what happens when capillary rheometry is used in the shear rate region where the instability–failure phenomenon had been observed with rotational rheometers. As previously reported, with a capillary rheometer, steady-state flow was observed at the very high shear rates.[12] However, the data at the low shear rates were excessively scattered and nonreproducible. We are going to explore the cause of the apparent anomaly. Another objective is to find mechanisms of flow through a capillary at superhigh shear rates.

EXPERIMENTAL

Samples

Three plastisol samples designated as 94, 96, and 98 were prepared with PVC (PVC 124A type resins, Poly-One Corp., Avon Lake, OH). The particle concentration was 52.8% volume fraction. The detail of the for-
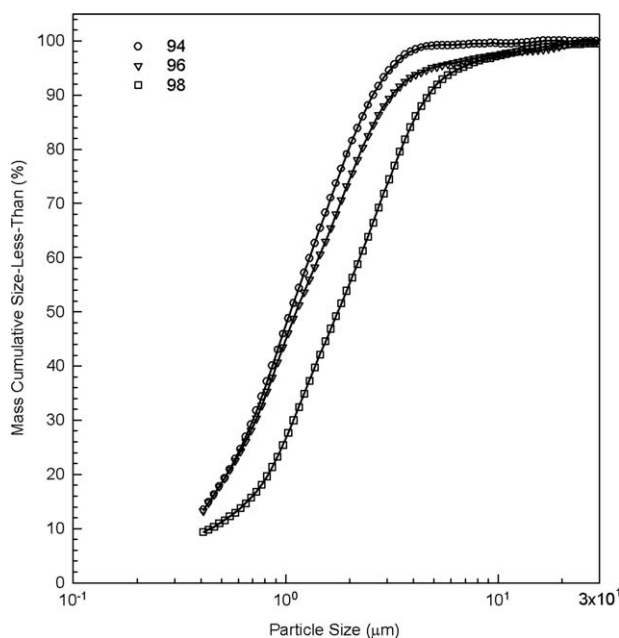

Figure 1 Cumulative mass distribution of the particles in the plastisols.

mulation was given in a previous paper.[12] The same resin was used for 94 and 96, but plastisol 96 contained 14% more emulsifier than 94. The resin used for 98 had an average particle size approximately twice as large as that for 94. The particle size distribution was about the same in both resins, as shown in Figure 1.

The emulsifier concentrations in 94 and 98 were the same.

Instrument and operation

The capillary rheometer (Sieglaff-McKelvey rheometer, Tinius-Olsen Testing Machine Co., Wallingford, CT) was a controlled-stress type, the length-to-diameter ratio was 49.8, and the diameter was 0.0255 cm. The very small diameter was necessary to generate high enough shear stress with this equipment in order to provide a superhigh shear rate approaching 10^5 s^{-1}. The data were corrected for the friction of plunger, affecting mostly the low shear stress measurements.

A Rheomeric model RDSII mechanical spectrometer (Rheometric Mechanical Spectrometer, TA Instruments, New Castle, DE) was used with a coaxial cylinder for the shear rate range of 10^{-1} to 3×10^2 s^{-1}. The length of the bob was 25.0 mm, and the diameters of the cup and bob were 50.0 and 48.0 mm, respectively.

The temperature of testing was 27°C for both rheometers.

RESULTS

The results are shown in Figure 2(a,b) as a plot of viscosity versus shear rate and that of shear stress versus shear rate, respectively.
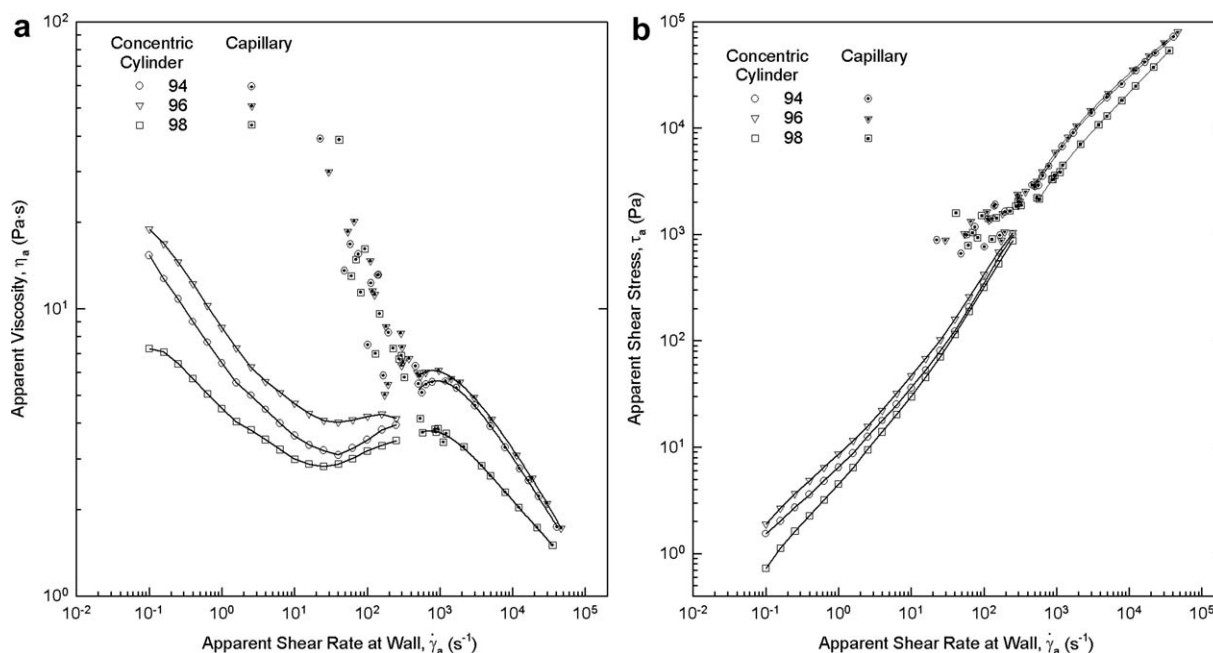
Figure 2 (a) Viscosity–shear rate relation and (b) shear stress–shear rate relation of the PVC plastisols observed with capillary and concentric cylinder rheometers.

In these plots, capillary data are shown for the shear rate range of about 20 to 40,000 s^{-1}. Also, the concentric cylinder rheometer data are shown for comparison. Because of the instability accompanying concentric cylinder measurements and the reproducibility problem of capillary measurements, the shear rate ranges of the two instruments could not be made to overlap. Even though the steady-state data from the two instruments may appear to match, if the two curves are extended, there is a discontinuity in the shear rate range. The nature of the discontinuity is one of the major questions addressed in this work.

With respect to the capillary data in the shear rate range of about 20 to 400 s^{-1}, the data points were excessively scattered (region I). Also, the viscosity and shear stress were much higher than those observed with the concentric cylinder rheometer. In the shear rate range between about 500 and 40,000 s^{-1}, the data were reproducible. The viscosity increased to a maximum (region II) and then decreased (region III) with the increase of shear rate. We shall discuss the capillary flow behavior for the three regions separately.

DISCUSSION

In region I, the scattering of the data might be attributable to instrumental and operational causes because stress-levels are low, approaching the resolution limits of the instrument. However, there is a possibility that the data-scatter may originate from

the nature of the material. With the rotational rheometer, a single charge of sample is used to obtain the viscosity data at different shear rates. With the capillary rheometer, the sample liquids going through the capillary at different shear rates come from different portions of the sample within the reservoir. The scattering of viscosity data in the present case quite possibly comes from the inhomogeneous nature of the sample. The capillary diameter is 255 μm, and the largest particle is about 15 μm, about 6% of the capillary diameter. If the variation in particle size is affecting the scattering of the data, the scattering should persist at the higher shear rate also.

In the quiescent state, the plastisol forms a dense network consisting of the particle chains.[13] Both large particles and small ones become part of the chain, instead of small ones residing in the interstice of large particles.[13] The sample shows yielding, and the flow behavior is somewhat dependent upon the previous mechanical history. The foregoing interpretation is proposed as a model for the flow behavior, which is assumed to be intimately related to the nature of the particle network. It is hoped that the model would lead to the understanding of the low-shear behavior of plastisol with respect to the resin type and plastisol formulation.

With reference to Figure 2(a,b), the effects of the particle size (94 vs. 98) and that of the emulsifier concentration (94 vs. 96) are not obvious because of the scattering of the data. If the scattering of the data were caused by the jamming of particles at the entrance of the capillary, a significant pressure loss

would have been observed. The jamming should have occurred at the higher shear rates also. Neither was the case.

Because the capillary data display much higher flow resistance than those obtained with the concentric cylinder rheometer, this fact indicates that the stress-induced phase separation did not occur within the capillary rheometer. Whereas the plastisol in the concentric cylinder rheometer can be separated into layers of the immobilized zone and the flowing zone, such a separation is difficult to materialize in a capillary, where the shear rate varies from zero at the center to a maximum at the capillary wall.

However, the high viscosity alone can not explain the scattering of the data. The problem of reproducibility may be related to the nature of the particle network[13] in the reservoir.

In order to flow into the capillary, the network must be broken or disrupted into fragments consisting of particles and occluded plasticizer. If the fragment becomes a flow unit and acts as if it were a particle, the observed viscosity would be higher than that expected for the concentration of particles because the total volume of the particle includes occluded plasticizer.

Even though the viscosity data are scattered, the general trend in viscosity value is to decrease with the increase of shear rate. This implies that the fragments break down (on the average) to a smaller size with the increase of shear rate.

Although it is difficult to estimate the fragment size, a relative size (average) may be estimated in terms of the occluded plasticizer as before[10] because the larger fragment contains more occluded plasticizer.

The fraction of occluded plasticizer (OP %) may be calculated through the following sequence.

Johnston and Brower[14] examined a large number of data on the viscosity of PVC plastisol as a function of the volume fraction (ϕ) of particles. The result was the development of a master curve in a form of log η_r as a function (F) of ϕ/ϕ_c:

$$\text{Log } \eta_r = F(\phi/\phi_c) \tag{1}$$

where η_r is the relative viscosity (ratio of the viscosity of plastisol to that of the plasticizer) and the symbol ϕ_c is the highest volume fraction of particles where the viscosity approaches infinity. In the present case, the volume fraction includes occluded plasticizer so that it is designated hereafter as ϕ_{app}. If the value of ϕ_c is known, ϕ_{app} may be calculated from the observed value of viscosity. However, the value of ϕ_c is unknown for the viscosity data obtained with the capillary rheometer. The ϕ_c previously estimated from viscosity with the rotational viscometer cannot be used because the flow mechanism is different. For reference, we used the viscos-

ity at a particular shear rate where fragments are assumed to be completely broken down to a single particle (the viscosity maximum in region II). From the observed value of viscosity, the estimated value of ϕ_c is 0.74. Although the actual value may be somewhat sample dependent, the difference could not be detected. The value of the viscosity of the plasticizer containing stabilizers (η_s) used for this calculation was 0.057 Pa s.[12]

The volume fraction of the occluded plasticizer is $\phi_{app} - \phi$, expressed as OP %, as

$$\text{OP\%} = [(\phi_{app} - \phi)/(1 - \phi)] \times 100 \tag{2}$$

The OP % data are plotted as a function of shear rate for region I and are shown in Figure 3(a–c) for samples 94, 96, and 98, respectively.

All the points fall approximately within the two limits; two lines are drawn in the figures in order to help visualize a trend of the data scatter of one sample against that of the other Several characteristics may be cited for the figures:

1. In spite of the scattering of the data, the overall trend is that the fragments become smaller with increasing shear rate.
2. The upper line, representing the largest amount of occluded plasticizer, corresponds to the largest size of fragments and the highest viscosity. The lower line represents the smallest amount of occluded plasticizer and corresponds to the smallest size fragments and the lowest viscosity. At any given shear rate, the average fragment size varies approximately within the two limits.
3. The variation of the fragment size increases with increasing shear rate.
4. The variation of the fragment size is like that of fragment size in fractured solids. It presumably comes from a nonuniform distribution of the weak points within the material. The preexisting network consisting of a variety of particles must be nonuniform in its local strength, for example, with respect to the number of contact points.[13]
5. The ranges of the data scatter in Figure 3(a,b) are almost identical. The ϕ_{app} range for 96 is only slightly higher than that for 94, the fact that is related to the corresponding differences of viscosity. The range for 98, shown in Figure 3(c), is very different from those of the other two [Fig. 3(a,b)]. The particle network consisting of the larger particles is different in the mode of fracture or in the amount of the occluded plasticizer. The type of plot like Figure 3 may be used to characterize (fingerprint) the particle network with respect to variables such as particle size and distribution; size,
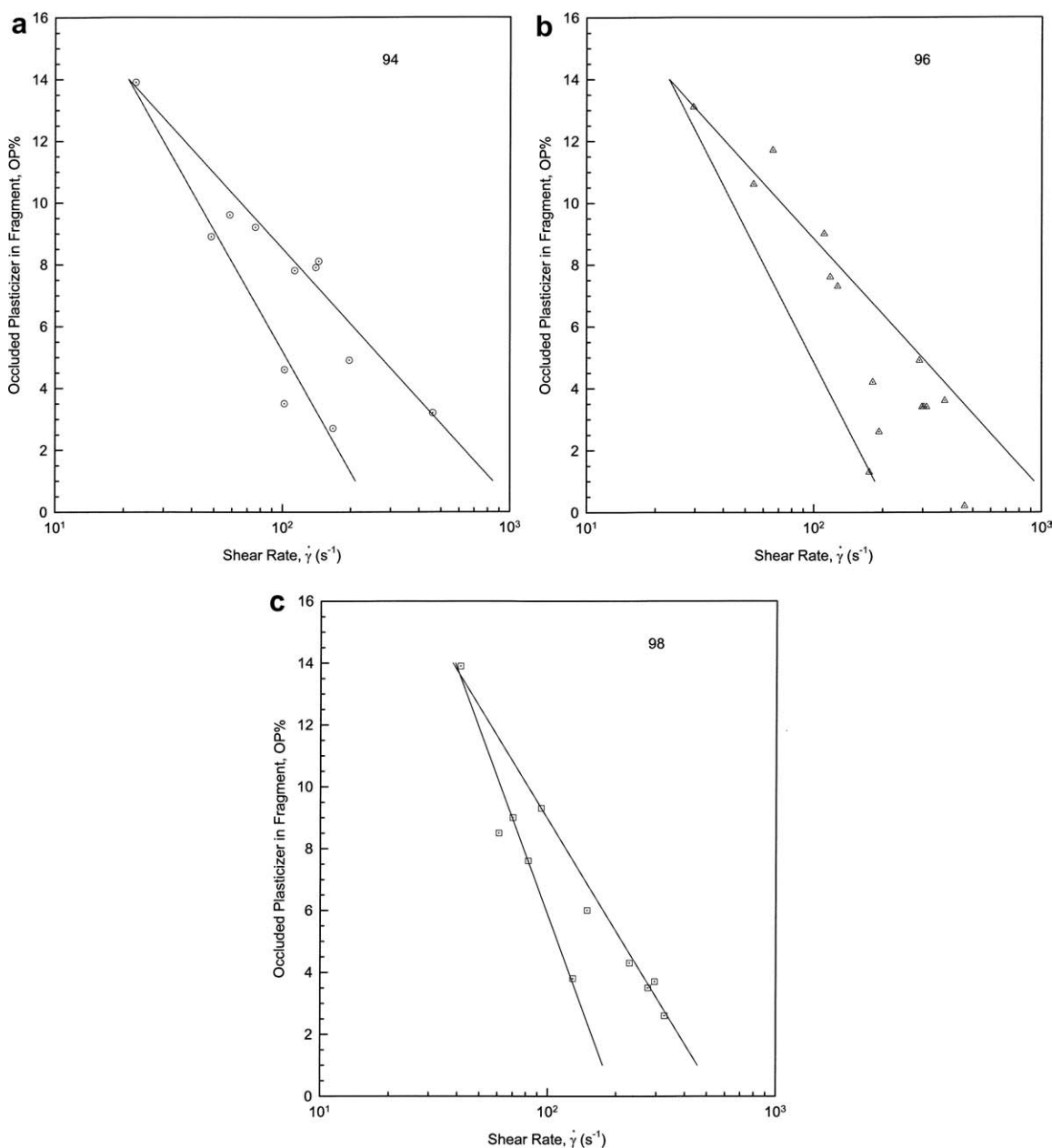
Figure 3 Occluded plasticizer in network fragments flowing through a capillary: samples (a) 94, (b) 96, and (c) 98.

shape, and friability of agglomerated particles; plasticizer type; type and amount of emulsifier; and other additives.

When the fragments become very small, the variation of size diminishes. Consequently, the viscosity data becomes more reproducible. This corresponds to region II, where the viscosity increases with increasing of shear rate. This is because small fragments play two opposite roles. Even though the occluded plasticizer increases the viscosity, the fragments, being larger than single particles, decrease the viscosity. If the latter effect dominates, the viscosity increases as more and more fragments break up into single particles. The amount of the occluded plasticizer, which was calculated from the viscosity, is listed in Table I.

The highest shear rate in the table is that where the viscosity maximum occurs. At this shear rate, OP % must be zero. The small nonzero number shown in the table is within the error of calculation. Also, in region II, there is some scattering of the data (see Fig. 2), which contributes to the error. Therefore, the OP % in the table is for showing the trend only.

In region III, there are no fragments, and each particle is separated from the others. Under the extremely high shear rate, the rotation of particles

TABLE I
OP % in Region II

	Sample				
94		96		98	
Shear rate (s^{-1})	OP %	Shear rate (s^{-1})	OP %	Shear rate (s^{-1})	OP %
510	2.1	493	2.7	535	0
1200	2.1	961	2.9		
3030	0.8	1880	2.3		

becomes difficult because the rotation generates interparticle shear field, resulting in an enormous flow resistance. When the rotation ceases, the behavior becomes plug flow with a thin layer of plasticizer lubricating the capillary interface. The thickness of the lubricating layer (ΔZ) was calculated in the following sequence.

First, the volume flow rate (Q) was calculated from the apparent shear rate ($\dot{\gamma}$) as

$$Q = \dot{\gamma}(\pi R^3/4) \tag{3}$$

where R is the radius of the capillary. Then, the relative velocity of the plug against the capillary wall (ΔU) was calculated from

$$\Delta U = Q/\pi R^2 \tag{4}$$

The shear rate of the lubricating layer ($\dot{\gamma}_L$) is

$$\dot{\gamma}_L = \tau/\eta_s \tag{5}$$

where τ is the shear stress and η_s is the viscosity of the plasticizer (plus stabilizers).

Finally

$$\Delta Z = \Delta U \dot{\gamma}_L \tag{6}$$

ΔZ is shown in Figure 4 as a function of shear rate. There are sample dependences in the relation, as they are expected from the viscosity curves shown in Figure 2(a).

A significant observation with the figure is that ΔZ matches the particle size of a given sample. This is shown in Table II.

There is no rigorous rationale to choose the particle size at 50% cumulative mass as the average particle size, but only an approximate measure of size is sufficient to interpret the present observation. Similarly, there is no precise reason to use constant shear stress for comparing the ΔZ values of different samples. Nevertheless, the data indicate that the particle size has an influence in controlling ΔZ. The formation of the lubricating layer must require both shear-induced exudation of plasticizer towards the
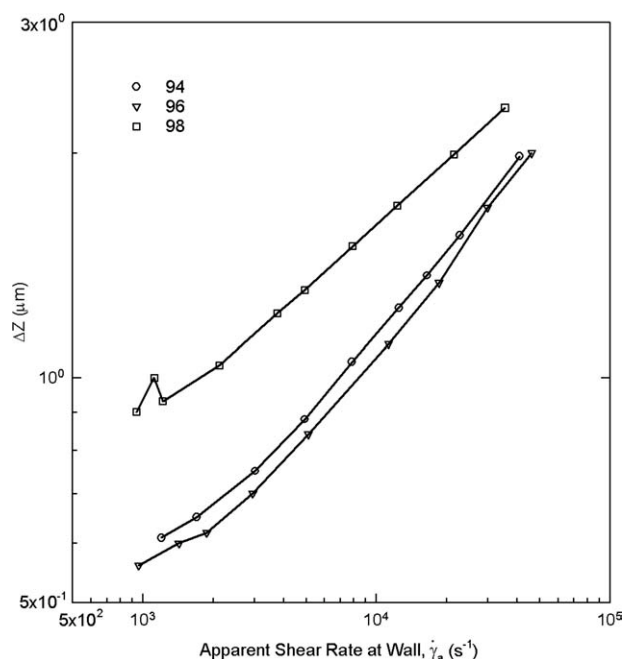
Figure 4 Estimated thickness of the lubricating plasticizer layer between the plug and capillary wall.

capillary wall and expulsion of particles from the proximity of the capillary wall.

Although the magnitude of the viscosity of the three samples follows the same order from high to low (96, 94, 98), at both below and above the instability, the mechanisms of the flow in the two regions are entirely different.

CONCLUSIONS

In the pseudo-plastic region (low to medium shear rates), the mechanism of flow of plastisol through a capillary die and that in a concentric-cylinder

TABLE II
Particle Size and ΔZ

	Sample		
	94	96	98
Average particle size μm (ratio of size)[a]	1.08 (1.00)	1.15 (1.06)	1.75 (1.62)
Thickness of layer μm (ratio of thickness)			
Shear stress (Pa)			
6,000	0.58 (1.00)	0.56 (0.97)	1.00 (1.72)
10,000	0.67 (1.00)	0.60 (0.90)	1.20 (1.56)
15,000	0.77 (1.00)	0.71 (0.92)	1.35 (1.75)
20,000	0.90 (1.00)	0.82 (0.91)	1.55 (1.72)
30,000	1.15 (1.00)	0.98 (0.85)	1.85 (1.61)
40,000	1.35 (1.00)	1.20 (0.89)	2.10 (1.56)
50,000	1.50 (1.00)	1.40 (0.93)	2.20 (1.47)
60,000	1.70 (1.00)	1.60 (0.94)	2.40 (1.41)

[a] Particle size at 50% cumulative mass counted from smaller to larger size.[12]

rheometer are different. In the latter, the mechanism is a stress-induced phase separation, and the growth of the immobilized phase accounts for the decrease of viscosity with the increase of shear rate. In the former, the phase separation does not occur. Also, fragments of the preexisting network of particle chains are carried through the capillary. Consequently, the observed viscosity with a capillary rheometer was much higher than that with a concentric cylinder rheometer. In the capillary, the fragments become smaller with increasing shear rate, resulting in a decrease of viscosity. The size of the fragments are not uniform, the fact that produced scattering of the observed viscosity. At high shear rates, the fragment-size becomes small and uniform, such that viscosity is reproducible. The flow is dilatant, and the viscosity reaches a maximum. In the superhigh shear rates, particles are separated from each other but cease rotating. The mechanism is plug flow with a thin layer of plasticizer lubricating the interface between the plug and the wall of the capillary. ΔZ increases with increasing shear rate but corresponds approximately to the average particle size of a given sample. The formation of the lubricating layer requires both shear-induced exudation of the plasticizer towards the wall and expulsion of particles from the vicinity of the wall.

References

1. Davidson, J. A.; Gardner, K. L. In Kirk–Othmer Encyclopedia of Chemical Technology, 3rd ed.; Wiley: New York, 1983; Vol. 23, p 922.
2. Brighton, C. A.; Marks, G. C.; Benton, J. L. In Encyclopedia of Polymer Science and Technology: Wiley: New York, 1971; Vol. 14, p 370.
3. Nakajima, N.; Daniels, C. A. J Appl Polym Sci 1980, 25, 2019.
4. Nakajima, N.; Ward, D. W. J Appl Polym Sci 1983, 28, 807.
5. Nakajima, N.; Harrell, E. R. Adv Polym Tech 1986, 6, 409.
6. Nakajima, N.; Harrell, E. R. J Elast Plast 2009, 41, 277.
7. Nakajima, N.; Harrell, E. R. J Appl Polym Sci 2007, 103, 2769.
8. Hoffman, R. L. Trans Soc Rheol 1972, 16, 155.
9. Nakajima, N.; Harrell, E. R. J Colloid Interface Sci 2001, 238, 116.
10. Nakajima, N.; Harrell, E. R. J Colloid Interface Sci 2001, 241, 492.
11. Nakajima, N.; Harrell, E. R. J Appl Polym Sci 2007, 103, 2769.
12. Nakajima, N.; Harrell, E. R. J Appl Polym Sci 2010, 115, 3605.
13. Nakajima, N.; Harrell, E. R. J Colloid Interface Sci 2002, 254, 362.
14. Johnston, C. W.; Brower, C. H. Soc Plast Eng J 1970, 26, 31.